



Cite this: *Mol. Syst. Des. Eng.*, 2022, **7**, 1039

Received 27th May 2022,  
Accepted 2nd August 2022

DOI: 10.1039/d2me00102k

[rsc.li/molecular-engineering](https://rsc.li/molecular-engineering)

**A modular platform for 3D printing fluid-containing structures is reported. Pickering emulsion-templated fluid-filled polymeric capsules were synthesized and incorporated into viscous liquids to produce inks for direct ink writing. Printed objects could be cured by solvent removal or irradiation with ultraviolet light to give monolithic structures containing capsules of fluid, with porosity dependent upon the curing method.**

## Introduction

The encapsulation of active liquids has found widespread application in drug delivery,<sup>1</sup> personal care,<sup>2</sup> energy management,<sup>3–5</sup> and consumer goods,<sup>6</sup> among other industries. Encapsulation is a protective technique in which a core material is isolated from its external environment by containment within a shell material. This process lends thermal stability to the encapsulate, along with resistance to leaching and defense against reaction with external agents. Further, encapsulation resolves challenges associated with bulk active liquid processing (*e.g.*, high viscosity) and increases the active surface area, which may aid in the mass transfer of small molecules across the interface.<sup>7</sup> Encapsulation can be accomplished by physical methods (*e.g.*, spray-coating) or chemical processes (*e.g.*, interfacial polymerization in emulsions).<sup>8,9</sup> Encapsulation of fluids enables their handling as solid powders which can facilitate their use in new applications – namely, as rheology modifiers for 3D printable materials.

3D printing (3DP), or additive manufacturing, is a method of producing three-dimensional objects from a feedstock

# Additive manufacturing: modular platform for 3D printing fluid-containing monoliths†

Ciera E. Cipriani,<sup>a</sup> Nicholas C. Starvaggi,<sup>b</sup> Katelynn J. Edgehouse,<sup>b</sup> Jordan B. Price,<sup>a</sup> Stephanie L. Vivod,<sup>c</sup> and Emily B. Pentzer<sup>\*ab</sup>

## Design, System, Application

Encapsulation of active liquids has found widespread application and can be used to protect a core material by isolating it from its external environment within a shell material. Encapsulation can also resolve challenges associated with bulk active liquid processing (*e.g.*, high viscosity) and increases the active surface area, which may aid in the mass transfer of small molecules across the interface, while also enabling the handling of fluids as solid powders which can facilitate their use in new applications – namely, as rheology modifiers for 3D printable materials. The 3D printing technique of direct ink writing (DIW) is advantageous for custom materials because it is inexpensive, simple to use, and ink composition can be readily modified to achieve desired rheological properties and material performance. Herein, we harness fluid-filled particles as rheology modifiers for DIW inks, thus introducing a modular platform for producing fluid-containing printed structures with modifiable matrices and particle fillers to achieve desired properties. We report two types of printable composite inks composed of viscous fluids and micron-scale particle fillers (capsules with a polyurea shell and core of liquid industrial lubricant poly( $\alpha$ -olefin)<sub>432</sub>, which was selected for its commercial availability and immiscibility with a variety of fluid matrices).

material. There are several methods to 3DP polymeric materials which use different feedstocks, including light-based techniques, like stereolithography and digital light processing, the powder fusion process of selective laser sintering, and extrusion methods such as fused filament fabrication and direct ink writing (DIW). Of the currently available 3DP technologies, direct ink writing (DIW) is advantageous for custom materials because it is inexpensive, simple to use, and ink composition can be readily modified to achieve desired rheological properties and material performance. DIW is a printing method in which a viscous, shear-thinning, thixotropic ink is extruded from a nozzle in a prescribed pattern. The ink is then solidified to form the desired object.<sup>10,11</sup> Particle fillers have previously been demonstrated to impart the necessary rheological properties to Newtonian liquids such as photopolymer resins<sup>12,13</sup> and polymer solutions<sup>14</sup> to prepare DIW inks. In this manner, the selection of polymer liquids and particle filler can be tuned

<sup>a</sup> Department of Materials Science and Engineering, Texas A&M University, 3003 TAMU, College Station, TX 77843, USA. E-mail: [emilypentzer@tamu.edu](mailto:emilypentzer@tamu.edu)

<sup>b</sup> Department of Chemistry, Texas A&M University, 3255 TAMU, College Station, TX 77843, USA

<sup>c</sup> NASA Glenn Research Center, 21000 Brookpark Road, Cleveland, OH 44135, USA

† Electronic supplementary information (ESI) available. See DOI: <https://doi.org/10.1039/d2me00102k>

to achieve desired functionality and performance of printed objects.

Previous efforts have been made to 3D print fluid-containing structures. These include impregnation of the printed geometry with fluid,<sup>15,16</sup> incorporation of liquid–solid core–shell particles into a printed substrate,<sup>17</sup> and printing of emulgels with a liquid phase which is stable to post-processing.<sup>18,19</sup> Specifically, fluid-filled particles have been directly printed, such as in the work by Acevedo and coauthors, who used direct laser writing to print solid shells which were then vacuum filled with liquid and sealed by printing a cap.<sup>15</sup> Rupp and Binder also harnessed the printed geometry to contain fluids within objects through a dual printing method where a fused deposition modeling extruder printed a poly( $\epsilon$ -caprolactone) (PCL) matrix, which was then filled with fluid using a liquid inkjet print head and enclosed by additional printed layers of PCL.<sup>16</sup> In an alternative technique, Lee and coauthors used stereolithography to print a poly(ethylene glycol)-diacrylate matrix, then harnessed coaxial electro-spraying to produce liquid–solid core–shell particles which were embedded in the printed matrix.<sup>17</sup> Although these methods have demonstrated promise in applications including drug delivery, nerve regeneration, and site-specific particle formulation, they have the limitation of requiring multiple feedstocks and thus multiple dispensers to produce printed objects. Zhang and coauthors complemented these previous efforts by developing Pickering

emulgels as a single feedstock for DIW printing. These emulgels were capable of containing a variety of materials within the dispersed phase, including liquid paraffin, which remained in printed structures after post-processing.<sup>18</sup> Pang and coauthors demonstrated the use of a similar DIW printable Pickering emugel system which contained sunflower oil.<sup>19</sup> Emulsions are useful for single-feedstock printing, but the interplay between dispersed phase, continuous phase, and surfactant identities and emulsion stability limits the composition of the inks. To complement these previous efforts, we sought to develop a process for printing fluid-containing structures using a single feedstock with modular composition.

Herein, we harness fluid-filled particles as rheology modifiers for DIW inks, thus introducing a modular platform for producing fluid-containing printed structures with modifiable matrices and particle fillers to achieve desired properties. We report two types of printable composite inks composed of viscous fluids and micron-scale particle fillers. Capsules with a polyurea shell and core of liquid industrial lubricant poly( $\alpha$ -olefin)<sub>432</sub> (PAO), were selected for commercial availability and immiscibility with various fluid matrices. These capsules were synthesized by the Pickering emulsion-templated interfacial polymerization process shown in Fig. 1A. One ink is a combination of a thermoplastic polyurethane (TPU) in *N,N*-dimethylformamide (DMF) solution and polyurea capsules filled with PAO. This ink is

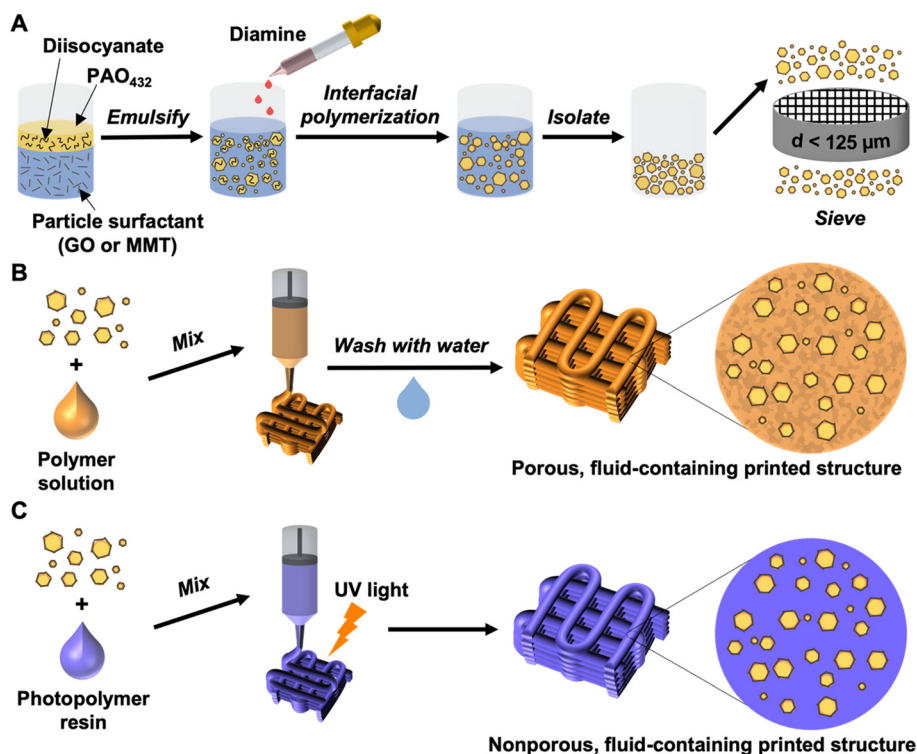


**Fig. 1** (A) Scheme of capsule synthesis, isolation, and sieving. (B) Combination of capsules and polymer solution, production and printing of ink, washing with water to remove solvent, and proposed porous microstructure. (C) Combination of capsules and photopolymer resin, production and printing of ink, irradiating with UV light to cure, and proposed nonporous microstructure.

printable by DIW and is cured by washing away solvent with water to produce porous, monolithic structures with desired geometries, as shown in Fig. 1B. The second ink is composed of a commercial liquid photopolymer resin as matrix and dark- or light-colored PAO-filled polyurea capsule fillers (Fig. 1C) which is also printed by DIW but cured by UV light. Ink rheology was evaluated using a parallel plate rheometer and monolithic structures containing PAO-filled capsules were 3D printed by DIW. Depth of cure experiments demonstrated that the color of the capsules dramatically impacted the curing of the resin by UV. All printed structures were examined by scanning electron microscopy (SEM), which elucidated porous or nonporous morphologies depending on the matrix. This work enables 3D printing of monolithic structures with desired geometries that contain pockets of fluid through a single printing step which yields composite materials for a variety of applications such as separations or selective delivery of active fluids.

## Results and discussion

PAO-filled polyurea capsules were synthesized using graphene oxide (GO) as a two-dimensional particle surfactant with Pickering emulsion-templated interfacial polymerization. GO was selected because of previous work demonstrating its

effectiveness for stabilizing oil-in-water emulsions.<sup>20–24</sup>

Optical microscopy images of the emulsion before polymerization are provided in Fig. S1† and demonstrate that the interface between the dispersed and continuous phases was successfully stabilized by GO. The resulting capsules, referred to as GO-C in this manuscript, were characterized by scanning electron microscopy (SEM), images from which are displayed in Fig. 2A. These images indicate that GO-C are spherical solid particles with diameters on the scale of tens of microns and slightly rough surfaces. To successfully incorporate GO-C into polymeric liquids to form printable inks, GO-C were sieved to remove particles with diameters  $>125\ \mu\text{m}$  and thus prevent clogging of the extrusion nozzle. Particle diameters of GO-C before and after this sieving were further characterized using laser diffraction particle size analysis, results of which are shown in Fig. S2.† The decrease in mean diameter from 53 to 39  $\mu\text{m}$  upon sieving, alongside the decrease in  $D_{90}$  from 89 to 62  $\mu\text{m}$ , indicates that large particles were successfully removed. The loading of PAO in the capsules was found to be approximately 75 wt% for unsieved and 80 wt% for sieved samples, as outlined in Table S1.† Upon mixing with a 1:10 w/v thermoplastic polyurethane (TPU):DMF solution at a weight ratio of 1:1.1 GO-C:solution, a viscous suspension was produced. This ink is referred to as GO-T and was printed into a lattice structure

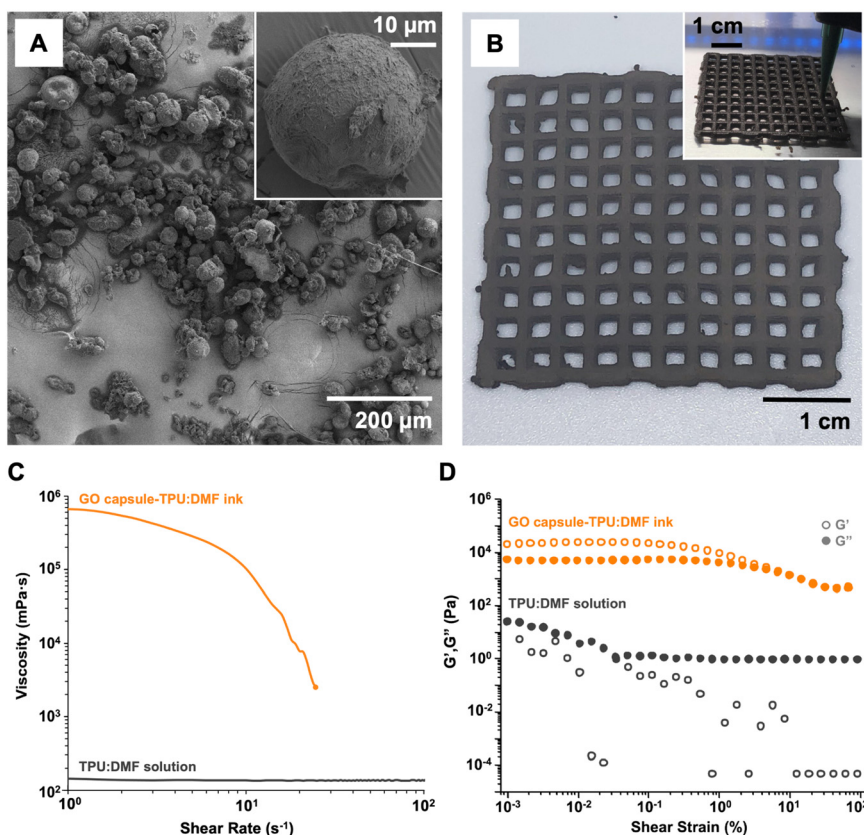


Fig. 2 (A) SEM images of GO-C. (B) Printed (inset) and cured lattice prepared from GO-T ink. (C) Shear rate-dependent viscosity of TPU:DMF solution (gray trace) and GO-T (orange trace). (D)  $G'$  and  $G''$  of TPU:DMF solution (gray markers) and GO-T (orange markers) as a function of shear strain.

(Fig. 2B, inset) and cured by washing with water to remove DMF, producing the solid, monolithic structure shown in Fig. 2B. Notably, the lattice was designed to possess horizontal dimensions of  $4 \times 4$  cm, and no macroscopic shrinkage was observed during the printing, curing, or drying. Individual printed filaments possessed cross-sectional diameters of approximately 1.2 mm (of note, varying the nozzle size could facilitate improved print resolution to print finely detailed structures). An additional image of the printing of GO-T, as well as SEM images of the surface of the printed lattice, are provided in Fig. S3.†

To further describe the printability of this suspension, the polymer solution and ink viscosities were measured over shear rates from 1 to  $1000 \text{ s}^{-1}$  (Fig. 2C and S4A.†). The TPU:DMF solution was found to be a Newtonian fluid, having a viscosity independent of the applied shear rate. Incorporating GO-C imparted non-Newtonian, shear-thinning behavior to the solution. Shear-thinning behavior is necessary for DIW inks so that a decrease in viscosity upon the application of the extruding force is observed, then the ink thickens after extrusion to hold the shape of the printed object until the ink is cured. Notably, at high shear rates, viscous suspensions tend to be expelled from the sides of the parallel plates of a rheometer in a manner characteristic of thixotropic materials; therefore, data were truncated at that point. The flow of the inks was also characterized by measuring the storage and loss moduli ( $G'$  and  $G''$ , respectively) across the shear strain range of 0.001 to 100% (Fig. 2D and S4B.†). Whereas the TPU:DMF solution flowed at all shear strains tested and did not exhibit a flow point (*i.e.*, a point at which  $G'$  and  $G''$  cross over one another), the GO-T ink behaved as a viscoelastic fluid with elastic behavior dominating at low strains and viscous behavior at high strains. The elastic behavior of GO-T results from interparticle interactions between capsules, which form a weak network to enable DIW printing of the ink. Specifically, steric stabilization, hydrogen bonding, and electrostatic forces cause the capsules to form flocs (*i.e.*, they aggregate).<sup>25</sup> Upon application of shear stress, these interparticle forces are overcome, and the flocs break apart. Increasing the applied stress further breaks down the flocs, resulting in the shear-thinning and yield stress behaviors observed in Fig. 2C and D. When the applied stress is ceased, the network of flocs is reformed.<sup>25,26</sup> The rheological characterization and printing of GO-T indicate that GO-C can serve as fillers in viscous liquids to produce inks which are printable by DIW. These inks can be cured by washing with water. 3DP with GO-T enables the production of fluid-containing monolithic structures with custom geometries in scenarios where water is readily available to wash away DMF, or where solvent evaporation is not of concern.

To make a truly modular 3DP platform, other polymer matrix materials and photocuring can be harnessed. A common class of 3DP materials are photopolymer resins, which are mixtures of liquid monomers/oligomers, photoinitiators, *etc.* The monomers/oligomers are

polymerized by irradiation with light, usually of UV wavelengths. To prepare a photocurable ink with fluid filled capsules, GO-C were mixed with a commercial photopolymer resin, Formlabs Elastic, to produce the ink GO-R which was printed by DIW, with UV light applied after each printed layer. Images of the printing and curing of GO-R at a layer height of 0.1 mm are shown in Fig. S5A and B,† respectively, and the resulting fully cured lattice is shown in Fig. S5C and D.† GO-R possessed the necessary rheological properties of a printable ink (Fig. S6.†), having similar performance to GO-T. However, the dark color of GO negatively impacted the ability of GO-R to fully cure at large layer heights. To mitigate this issue, polyurea capsules were synthesized using the same procedure as GO-C but using montmorillonite (MMT) clay as a particle surfactant. MMT was selected due to its light color and previous demonstrated use as an oil-in-water emulsion stabilizer.<sup>27,28</sup> Optical microscopy images of the MMT-stabilized emulsion are displayed in Fig. S7,† and interfacial polymerization led to PAO-filled capsules, called MMT-C. Particle size distributions for MMT-C before and after sieving to  $\leq 125 \mu\text{m}$  are provided in Fig. S8,† along with SEM images in Fig. S9,† both of which show slightly larger particle sizes than GO-C, although the wt% PAO core was nearly identical for GO-C and MMT-C ( $\sim 80$  wt%, Tables S1 and S2.†). Digital images of GO-C and MMT-C, along with the paste-like GO-R and MMT-R inks, are displayed in Fig. 3A and show that MMT-C produced a nearly white ink, whereas GO-C produced a dark brown ink. MMT-R was a printable, shear-thinning, viscoelastic fluid (Fig. S10.†). Images of the printing and curing of MMT-R at a layer height of 0.1 mm are shown in Fig. S11A and B,† respectively, and the resulting fully cured lattice is shown in Fig. S11C and D.† To quantify the effect of different colored particle additives on the curing process, vials were filled with the inks and irradiated with UV light

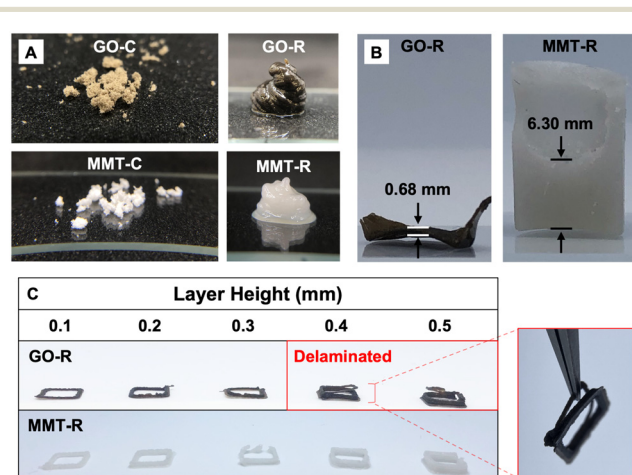
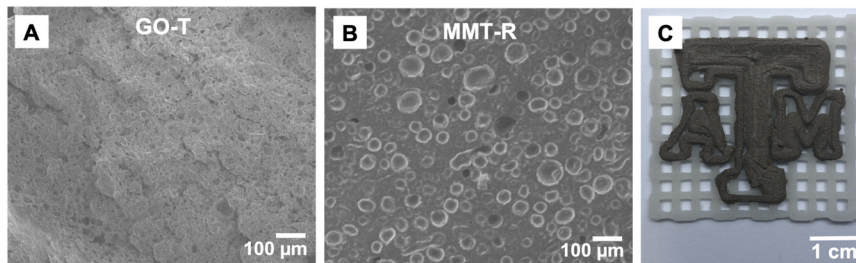


Fig. 3 (A) Digital images of GO-C, GO-R, MMT-C, and MMT-R. (B) Representative samples of GO-R and MMT-R after DOC experiment, with average DOC values shown. (C) GO-R and MMT-R samples printed using different layer heights and UV cured between each layer. Image on right shows delamination of GO-R sample printed using 0.4 mm layer height.



**Fig. 4** (A) SEM image of GO-T cross-section. (B) SEM image of MMT-R cross-section. (C) Assembled object, with lattice printed using MMT-R and Texas A&M University logo printed using GO-T.

from below for  $5 \times 30$  seconds. The average depth of cure (DOC) was over 9 times higher for MMT-R than GO-R, as shown in Fig. 3B and Table S3.† The dark color of GO-R prevented full curing of printed structures when layer heights were 0.4 mm or higher, whereas MMT-R enabled curing of structures even at layer heights of 0.5 mm. This is demonstrated by the delamination of GO-R layers at large layer heights, while MMT-R did not experience any delamination (Fig. 3C).

The successful printing of GO-T and MMT-R demonstrates that both the viscous liquid matrix and particle fillers can be exchanged to produce modular DIW inks and, thus, fluid-containing printed monoliths. Furthermore, the microstructure of the printed objects varies depending on the ink composition. The SEM images of the cross-section of printed GO-T shown in Fig. 4A and S12† indicate the porous microstructure of the TPU matrix, where GO-C are embedded within TPU, and void space is seen between the particle cross-sections. In contrast, photopolymer resin cures in a bulk solid state with no void space between particle cross-sections, as shown in Fig. 4B. These variations in microstructure influence the compressibility of the cured inks as reported in Fig. S13,† with GO-T having compressibility more similar to that of porous TPU than bulk TPU. MMT-R exhibited similar compressibility to pure photopolymer resin. Therefore, the ink composition influences the printing process, curing method, and resulting properties of the printed objects.

Depending on the polymer matrix and curing conditions, porous and nonporous structures are accessible through our modular printing platform. Furthermore, controlled release of fluids is facilitated by using different particle fillers and different matrices. This is demonstrated by the oil leakage over time of GO-T and MMT-R reported in Fig. S14.†  $1 \text{ cm}^3$  samples of the inks were printed, and their masses were measured over a 14 day period. GO-T experienced over a 50% mass loss in 7 days and then plateaued, whereas MMT-R had <1% mass loss over the two week period. We hypothesize that the porosity of GO-T enabled the release of PAO, while the nonporous MMT-R did not allow PAO to exit the printed structure. Multimaterial printing of such structures is also possible as shown in Fig. 4C, where MMT-R was used to print a lattice substrate, and the block T Texas A&M University logo was printed using GO-T. In the future, this could enable

morphological control of printed materials to enable location-specific access to fluids within capsules. Furthermore, in the present case, GO-C and MMT-C are both spherical particles with similar surface morphologies as seen in Fig. 2B and S9;† as such, the use of GO or MMT to form capsules should produce similar morphologies in printed structures. Other particles of different shapes, sizes, or surface textures could be harnessed to produce desired morphology variations within printed structures.

## Conclusions

In this communication, we report a modular platform for 3D printing objects which contain pockets of fluid by using fluid-filled capsules as rheological modifiers in two different polymer matrices. Micron-scale PAO-filled polyurea capsules were synthesized using GO as a two-dimensional particle surfactant and interfacial polymerization to produce a polyurea. These capsules were incorporated into a TPU:DMF solution to produce an ink which was printable by DIW and curable by solvent removal (*i.e.*, washing with water), yielding objects containing PAO and having micron-scale porosity. Alternatively, a photopolymer resin was used as a viscous liquid matrix, with PAO-filled capsules added as a rheological modifier. Light-colored capsules synthesized using MMT as a surfactant (rather than capsules dark in color from GO) enabled larger depth of cure using UV light. These UV-cured printed objects did not have micron-scale porosity and did not have leakage of the encapsulated PAO over 14 days. As such, the printing process and microstructures of printed objects can be tuned by changing the ink composition. Printing fluid-containing structures enables the handling of functional fluids as monolithic solids, which could prove useful in scenarios such as self-healing printed objects or selective delivery of active liquids, among other applications.

## Author contributions

E. P., S. V., and C. C. conceived the research. K. E. developed the GO-stabilized encapsulation procedure. N. S. developed the MMT-stabilized encapsulation procedure, synthesized all capsules, collected optical microscopy images, and performed the wt% core, particle size analysis, and compression experiments. J. P. developed the inks, performed the 3D

printing, performed the DOC experiments, performed the oil leakage measurements, and took digital images, and C. C. supervised. C. C. performed the rheology measurements and took SEM images. C. C. made all figures. C. C., N. S., and J. P. prepared the original draft, and all authors reviewed and edited. E. P. and S. V. supervised. E. P. acquired funding for the research.

## Conflicts of interest

There are no conflicts to declare.

## Acknowledgements

Use of the TAMU Materials Characterization Facility is acknowledged. Dr. Sisi Xiang and Dr. Yordanos Bisrat are acknowledged for providing SEM training and Dr. Wilson Serem for providing particle size analyzer training. Use of the Texas A&M University Soft Matter Facility (RRID:SCR\_022482) and DMA training by Dr. Peiran Wei are acknowledged. The authors also thank Dr. Peiran Wei for assisting with plotting particle size analysis data, alongside Chia-Min Hsieh for assistance with the oil leakage experiments. C. C. is supported by a NASA Space Technology Graduate Research Opportunity. E. P., K. E., J. P., and N. S. thank National Science Foundation Division of Materials Research grant #2103182 for funding.

## References

- 1 M. N. Singh, K. S. Y. Hemant, M. Ram and H. G. Shivakumar, *Res. Pharm. Sci.*, 2010, **5**, 65–77.
- 2 F. Casanova and L. Santos, *J. Microencapsulation*, 2016, **33**, 1–17.
- 3 E. M. Shchukina, M. Graham, Z. Zheng and D. G. Shchukin, *Chem. Soc. Rev.*, 2018, **47**, 4156–4175.
- 4 P. A. Advincula, A. C. De Leon, B. J. Rodier, J. Kwon, R. C. Advincula and E. B. Pentzer, *J. Mater. Chem. A*, 2018, **6**, 2461–2467.
- 5 Y. Yoo, C. Martinez and J. P. Youngblood, *ACS Appl. Mater. Interfaces*, 2017, **9**, 31763–31776.
- 6 B. F. Gibbs, S. Kermasha, I. Alli and C. N. Mulligan, *Int. J. Food Sci. Nutr.*, 1999, **50**, 213–224.
- 7 Q. Luo and E. Pentzer, *ACS Appl. Mater. Interfaces*, 2020, **12**, 5169–5176.
- 8 S. H. Sonawane, B. A. Bhanvase, M. Sivakumar and S. B. Potdar, in *Encapsulation of Active Molecules and Their Delivery System*, ed. S. H. Sonawane, B. A. Bhanvase and M. Sivakumar, Elsevier, 2020, pp. 1–8.
- 9 P. Wei, Q. Luo, K. J. Edgehouse, C. M. Hemmingsen, B. J. Rodier and E. B. Pentzer, *ACS Appl. Mater. Interfaces*, 2018, **10**, 21765–21781.
- 10 J. A. Lewis, *Adv. Funct. Mater.*, 2006, **16**, 2193–2204.
- 11 M. A. S. R. Saadi, A. Maguire, N. T. Pottackal, M. S. H. Thakur, M. M. Ikram, A. J. Hart, P. M. Ajayan and M. M. Rahman, *Adv. Mater.*, 2022, **34**, 2108855.
- 12 P. Wei, C. E. Cipriani and E. B. Pentzer, *Matter*, 2021, **4**, 1975–1989.
- 13 C. E. Cipriani, T. Ha, O. B. Martinez Defilló, M. Myneni, Y. Wang, C. C. Benjamin, J. Wang, E. B. Pentzer and P. Wei, *ACS Mater. Au*, 2021, **1**, 69–80.
- 14 P. Wei, H. Leng, Q. Chen, R. C. Advincula and E. B. Pentzer, *ACS Appl. Polym. Mater.*, 2019, **1**, 885–892.
- 15 R. Acevedo, M. A. Restaino, D. Yu, S. W. Hoag, S. Flank and R. D. Sochol, *J. Microelectromech. Syst.*, 2020, **29**, 924–929.
- 16 H. Rupp and W. H. Binder, *Adv. Mater. Technol.*, 2020, **5**, 1–8.
- 17 S.-J. Lee, W. Zhu, L. Heyburn, M. Nowicki, B. Harris and L. G. Zhang, *IEEE Trans. Biomed. Eng.*, 2017, **64**, 408–418.
- 18 Y. Zhang, G. Zhu, B. Dong, F. Wang, J. Tang, F. J. Stadler, G. Yang, S. Hong and F. Xing, *Nat. Commun.*, 2021, **12**, 111.
- 19 B. Pang, R. Ajdary, M. Antonietti, O. Rojas and S. Filonenko, *Mater. Horiz.*, 2022, **9**, 835–840.
- 20 S. C. Thickett and P. B. Zetterlund, *ACS Macro Lett.*, 2013, **2**, 630–634.
- 21 S. C. Thickett and P. B. Zetterlund, *J. Colloid Interface Sci.*, 2015, **442**, 67–74.
- 22 S. C. Thickett, N. Wood, Y. H. Ng and P. B. Zetterlund, *Nanoscale*, 2014, **6**, 8590–8594.
- 23 Y. Fadil, F. Jasinski, T. Wing Guok, S. C. Thickett, H. Minami and P. B. Zetterlund, *Polym. Chem.*, 2018, **9**, 3368–3378.
- 24 K. J. Edgehouse, N. Rosenfeld, D. E. Bergbreiter and E. B. Pentzer, *Ind. Eng. Chem. Res.*, 2021, **60**, 14455–14463.
- 25 H. A. Barnes, *A Handbook of Elementary Rheology*, University of Wales, Institute of Non-Newtonian Fluid Mechanics, 2000.
- 26 J. Mewis, *J. Non-Newtonian Fluid Mech.*, 1979, **6**, 1–20.
- 27 W. J. Ganley and J. S. van Duijneveldt, *Langmuir*, 2017, **33**, 1679–1686.
- 28 J. Dong, A. J. Worthen, L. M. Foster, Y. Chen, K. A. Cornell, S. L. Bryant, T. M. Truskett, C. W. Bielawski and K. P. Johnston, *ACS Appl. Mater. Interfaces*, 2014, **6**, 11502–11513.